HOT ROLLED HIGH STRENGTH CARBIDE-FREE 0.3%C BAINITIC STEELS WITH IMPROVED TOUGHNESS

Allain S. - Arcelor Research, Maizières les Metz, France
Caballero F.G. - CENIM-CSIC, Madrid, Spain
Santofimia M.J. - CENIM-CSIC, Madrid, Spain
Couturier A. - Arcelor Research, Maizières les Metz, France
Capdevila C. - CENIM-CSIC, Madrid, Spain
García de Andrés C. - CENIM-CSIC, Madrid, Spain
Iung T. - Arcelor Research, Maizières les Metz, France

ABSTRACT

An innovative concept based on theory alone has been followed to design new 0.3%C bainitic steels. The key idea is to adapt their compositions to reproduce the thermodynamical behavior, and thus the microstructure of given steel, which appears to be a benchmark for mechanical properties. The target microstructure is composed fine plates of upper bainitic ferrite separated by thin films of stable retained austenite, blocks of martensite but carbides are avoided by the judicious use of silicon. Seven alloys have been proposed after calculation and processed at a semi industrial scale. As expected, all the studied steels present quite similar but significant combinations of strength and ductility. Theirs UTS range from 1600 MPa to 1950 MPa while keeping a UEl = 4 % and a TEl > 10 %. Regarding toughness at room temperature, they match tempered martensitic steels, known to be the best-in-class regarding this property. The alloys present also a low YS/UTS ratio, which is beneficial for formability. Even if the concepts used for the alloy design are still controversial, the experimental results show that the targeted microstructure have been obtained in almost all grades altogether with the same superior mechanical compromises. The relative effects of the alloying elements are well taken into account and the model gives operational rules for element substitution for the alloy design of bainitic steels.

KEYWORDS

Bainite, UHSS, carbide, TRIP-Si, Multiphase, retained austenite

INTRODUCTION

The ‘typical’ thermomechanical process to produce bainitic steels has not been in practice as successful as those quenched and tempered, because the presence of coarse cementite particles in the bainitic microstructure [1,2]. The formation of cementite has at least two detrimental effects in the microstructure: (i) cementite particles are responsible for damage initiation in modern high-strength steels, and (ii) carbon is “lost” in cementite and cannot be utilized for precipitation strengthening. In medium carbon, the precipitation of cementite can be suppressed by alloying the steel with carbides inhibitors such as silicon and aluminum (>1 %). The carbon that is rejected from the bainitic ferrite enriches the residual austenite, thereby stabilizing it down to ambient temperature. The resulting microstructure consists of fine plates of bainitic ferrite separated by

HOME

carbon-enriched regions of austenite. There may also be some martensite present. These typical microstructures in medium carbon steels are called carbide-free bainite [2].

Their interests are manifold since these steels can combine high mechanical compromises with improved in-use properties, i.e. high tensile strength while keeping sufficient ductility for forming and showing a high resistance to damage. The high flow stresses are due to the absence of ferrite in the microstructure contrary to existing TRIP steels and to the low thickness of the bainitic laths. The TRIP effect expected from the residual austenite and the presence of islands of martensite lead to high instantaneous hardening rates. The in-use properties, such as toughness, resistance to damage, fatigue, sensibility to cut-edge and even weldability [3] are also noteworthy. The main advantages of these microstructures are exhaustively listed and detailed in [2]. The achieved combinations of properties are of great interest for the design of safety parts in the automotive industry. The main aim of this collaborative study funded by the ESCS program [4] is to develop hot-rolled carbide-free bainitic medium carbon steels with both high strength and high toughness (aiming finally to be less than 0.3%C at least for full-scale manufacture).

In general there are two ways of obtaining a bainitic microstructure: the first is to apply high cooling rates and multi stage cooling in the run-out table of the hot strip mill in order to allow the austenite to overcool into the bainite transformation range. The second alternative is the increase of steel hardenability. That means using an appropriate alloy design where elements like manganese and carbon retard the formation of allotriomorphic ferrite relative to the bainite reaction. A combination of both ways was here investigated in so far as the challenge of the activity thus consists in producing the targeted microstructure without deep alteration of the hot rolling route already used to produce TRIP steel. The Fig. 1 presents the most adequate processing route to obtain a full bainitic microstructure including a two-steps cooling suggested by the TTT diagrams [ ]. An initial rapid cooling should be performed to avoid the formation of proeutectoid ferrite during cooling. Afterwards and always before Ms temperature is reached, cooling should be slowed down in order to cross the bainitic zone of the TTT diagram. The secondary cooling stage after the FCT controls the bainitic transformation, the carbon enrichment of the austenite and the ratio martensite/retained austenite consequently.

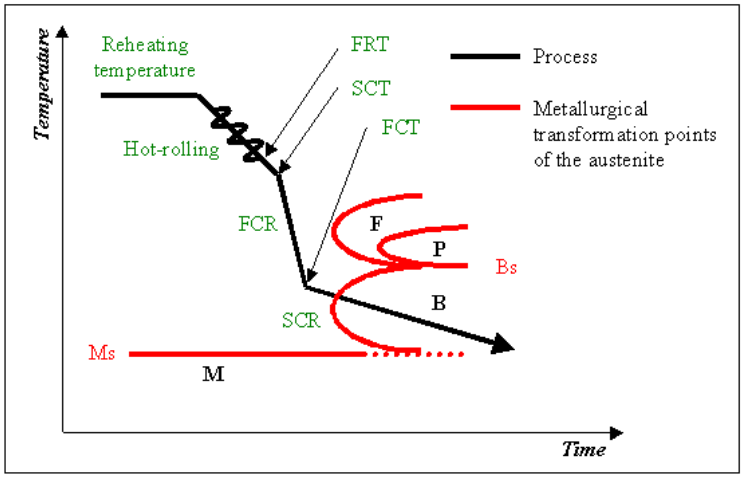

Fig. 1: Typical hot-rolling schedule used to obtain bainitic steels. The main reference temperatures are indicated on the thermal path (FRT = Finish Rolling Temperature, SCT = Start Cooling Temperature, FCR = First Cooling Rate, FCT = Finish Cooling Temperature, SCR = Secondary Cooling Rate, M = Martensite, F = Ferrite; P = Pearlite, B = Bainite). M_s and B_s are respectively the martensitic and bainitic transformation temperatures of the austenite.

Previous research, carried out by Bhadeshia and Edmonds [6,7] and Miihkinen and Edmonds [8,9,10], on two silicon-containing steels, nominally, Fe-0.2C-2Si-3Mn and Fe-0.4C-2Si-4Ni showed that these alloys hold promise. The Fe-0.2C-2Si-3Mn alloy exhibited excellent fracture toughness (KI c=125 MPa.$m^{1/2}$) in a yield strength range of 1000-1100 MPa as isothermally heat-treated between 350 and 300 °C. Because of the increased carbon content, higher strength levels 1200-1400 MPa were obtained in the Fe-0.4C-2Si-4Ni alloy, with lower fracture toughness values. In more recent research by Caballero et al. [11], bainitic 0.3%C grades have been elaborated. These alloys achieved elongation values of 14 % for strength in the range of 1600-1700 MPa and a good toughness (Kic = 130 MPa.$m^{1/2}$). The composition of the most promising grade called Ni2 in the following is given the Table 1.

The main idea of the current project is of fundamental nature. It consists in trying to reproduce the microstructure of the Ni2 steel with a lower content of alloying elements. As the consequence, the same highest or even better mechanical properties are supposed to be reached. For these purpose, it has been assumed that if two alloys have the same transformation points upon cooling, they will exhibit more or less the same microstructure after a given thermomechanical processing. Seven chemical compositions have thus been customized in such way using a thermodynamic model. The carbon content has been fixed at 0.3%C.

1. ALLOY DESIGN

The first step of this work is the design, using phase transformation theory, of a series of carbide free bainitic steels, given a set of industrial constraints. The incomplete reaction phenomena or T_0' concept has been used to optimize the microstructure by increasing the amount of bainitic ferrite in order to minimize the presence of blocks of austenite. For this purpose, we used the thermodynamic model developed by Bhadeshia [12], which predicts the T_0' curve and the TTT diagram from the chemical composition of the steel. The intention of this work is not to discuss the fundamentals of the bainitic transformation here. We only benefit from the existing thermodynamical theory and model. As the consequence, we here suppose that the bainite transformation progresses by the diffusionless growth of tiny platelets known as "sub-units". The excess carbon in these platelets partitions into the residual austenite soon after the growth event. Diffusionless growth of this kind can only occur if the carbon concentration of the residual austenite is below that given by the T_0' curve. The T_0' curve is the locus of all points, on a temperature versus carbon concentration plot, where austenite and ferrite of the same chemical composition have the same free energy taking into account an empirical contribution due to strain energy in bainitic ferrite. It follows that the maximum amount of bainite that can be obtained at any temperature is limited by the fact that the carbon content of the residual austenite must not exceed the T_0' curve on the phase diagram [13,14,15,16]. The T_0' concept can be used to minimize the amount of blocky, unstable austenite present in the microstructure [6,7]. An increase in the amount of bainitic ferrite in the microstructure is needed in order to consume the blocks of austenite.

Predictions give us an initial idea of important parameters and properties such as transformation temperatures, hardenability and maximum volume fraction of bainite formed at a given temperature. Special attention have thus been paid to the following parameters:

- t_d, which represents the time at the ferrite and pearlite nose in the TTT diagram;
- t_{ad}, which represents the time at the bainitic nose in the TTT diagram;
- V_{B400}, which indicates the maximum volume fraction of bainite formed at 400ºC according to the T_0' curve.
- M_s martensite start temperature

- B_s bainite start temperature

The new alloys were designed to have t_{ad} and $V_{B\ 400}$ parameters similar to those of Ni2 steel designed in previous work [11]. Moreover, the t_d values of the new alloys must be high enough to avoid the formation of proeutectoid ferrite during cooling. Table 1 shows the chemical composition of the reference Ni2 steel and the new designed grades.

Table 1: Composition of the steels designed for the purposes of the study. The values have to be compared to those given for the Ni2 reference steel. The compositions of the new alloys permit to reproduce the TTT and T_0' curves of the Ni2 steel. The only noticeable difference in the calculated thermodynamical behavior concern the diffusionnal transformation (t_d). The meanings of the parameters are given above.

Ref	C	Mn	Si	Al	Cr	Ni	Mo	Co	t_d (s)	t_{ad} (s)	V_{B400}	M_s (°C)	B_s (°C)
Ni2	0.30	1.50			1.44	3.50	0.25		570	14	0.43	334	420
#1	0.30	2.23	1.50				0.25		56	14	0.44	333	420
#2	0.30	2.00	1.50		0.46		0.25		50	14	0.44	335	420
#3	0.30	1.50	1.50		1.46		0.25		41	14	0.44	333	420
#4	0.30	1.50	1.50		0.17	1.50	0.25		160	14	0.44	334	420
#5	0.30	2.00	1.50		1.16		0.25	1.00	64	14	0.44	334	420
#6	0.30	2.00	1.50		1.51		0.25	1.50	70	14	0.44	334	420
#7	0.30	2.00	1.50	1.00	1.51	1.76	0.25	1.50	120	14	0.44	334	420

The C and Mo contents of all the alloys were fixed to those in the reference Ni2 steel. A silicon content of 1.5 wt.% is at least required to suppress carbide precipitation. Mo addition is made to reduce impurity embrittlement and to increase hardenability. Steel #1 has been proposed as a reference. The potential effect of chromium will be studied with the help Steel #2 and #3. It is known that nickel is an alloying element used to increase the toughness and tensile strength without detrimental effect on the ductility. In this sense, Steel #4 has been designed by adding 1.5 Ni to a 0.3C-1.5Mn-Cr based alloy and its Cr content was reduced in order to reach the same t_{ad} and V_{B400} than those in Ni2 steel. This alloy is useful to study how the Ni affects the microstructure and toughness itself by comparison to the other designed alloys. Recent studies [17] on high carbon high silicon bainitic steels have shown that the addition of Co and Al increases the maximum volume fraction of bainitic ferrite and reduces the thickness of ferrite plates refining the microstructure. With the aim of studying the influence of both elements, Steels #5, #6 & #7 were proposed.

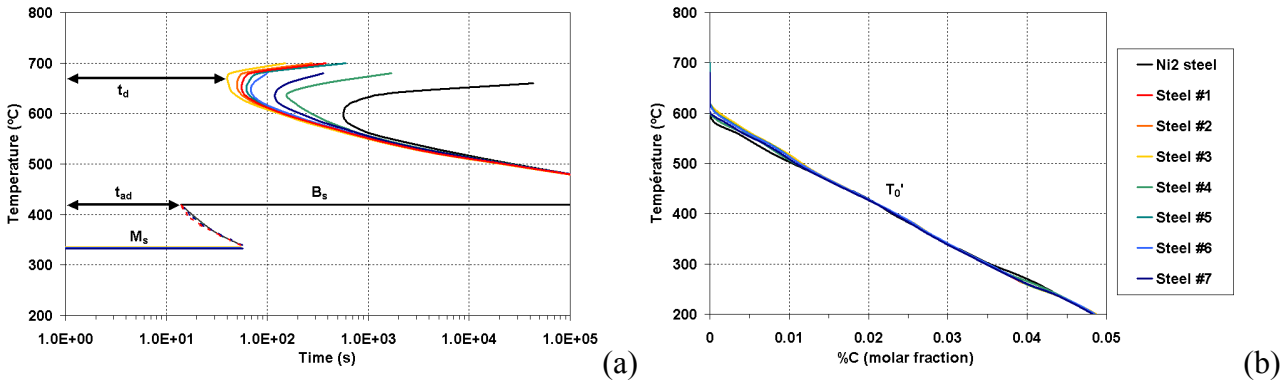

Fig. 2: (a) Calculated TTT curves of the new designed alloys and the reference Ni2 steel. (b) T_0' curves as calculated by the thermodynamical model under an isothermal holding.

Fig. 2 shows the TTT diagram and the T_0' curves of the designed steels in comparison with those for Ni2 steel. TTT diagrams show that all the new alloys have similar diffusionless curves and B_s

and M_s temperatures, but different diffusional noses. Moreover, the T_0' curve of the different steels match perfectly. This is not surprising since those alloys have been designed to have the same maximum volume fraction of bainite at 400°C.

TTT diagrams presented Fig. 2a confirm that a two-steps cooling is the most adequate processing route to obtain a full bainitic microstructure in the new alloys. An initial rapid cooling should be performed to avoid the formation of proeutectoid ferrite during cooling. Afterwards and always before B_s temperature is reached, cooling should be slow down in order to cross the bainitic zone of the TTT diagram.

Finally, kinetics models for bainite transformation described elsewhere [5] were used to estimate the volume fraction of bainite formed by different cooling routes. The input values in these models are: the chemical composition (C, Si, Mn, Cr, Ni, V and Mo), the prior austenite grain size and the cooling route. The influence of Co and Al in the transformation is not included in this calculation. According to the modeling a full bainitic microstructure (volume fraction of bainite higher than 80 %) will be formed applying the following manufacturing procedure: FRT = 925 ºC; FCR = 30 ºC/s; FCT = 600 ºC; second cooling rate: 0.5 ºC/s. An intermediate solution between this previous one and direct quenching has been retained to perform the experiments. The aimed hot rolling schedule is: FRT > 900 ºC; FCR > 50 ºC/s; FCT = 500 ºC followed by an air-cooling. The secondary cooling rate is then more or less equal to 0.5°C/s.

2. EXPERIMENTAL PROCEDURE

All the laboratory heats were elaborated using a 60kg vacuum induction furnace under inert atmosphere (Ar, N2). The generator power is 80kW. Pure (>99.9%) electrolytic iron and addition of the alloying elements one after each other were used. Carbon desoxydation was performed and an analysis of C, S, N, O was made on line during elaboration for the final adjustment of composition. During elaboration, the temperature is controlled by a thermocouple. The final compositions of the ingots have controlled and the results are given the Table 2. Except for the silicon content in Steel #4 the compositions of the elaborated steels match with those proposed in the Table 1. This discrepancy will have neither relevant impact on mechanical properties or on phase transformations.

Table 2: Compositions and processing parameters followed for the elaboration of steels. The chemical compositions are close to those proposed in the table 1 except for steel #4 who Si content is slightly too high. The processing parameters have been followed closely. The only discrepancy has been obtained for the FCT of the first attempt.

References		Composition								Hot-rolling schedule		
Grade	FCT (°C)	C	Mn	Si	Al	Cr	Ni	Mo	Co	FRT (°C)	FCR (°C/s)	FCT (°C)
#1	500	0.285	2.25	1.5	0	0	0	0.255	0	904	77	440
	600									904	45	586
#2	550	0.29	1.97	1.46	0	0.455	0	0.25	0	900	48	550
	500									913	60	490
#3	550	0.285	1.56	1.49	0	1.47	0	0.245	0	913	50	563
	500									913	53	504
#4	500	0.27	1.53	1.71	0	0.17	1.47	0.245	0	928	86	514
#5	550	0.285	1.97	1.47	0	1.2	0	0.245	0.97	895	46	560
	500									905	55	494
#6	500	0.285	2.04	1.5	0	1.5	0	0.245	1.48	933	75	516
#7	500	0.3	2.06	1.44	1.01	1.6	1.7	0.24	1.43	905	64	504
	600									927	45	609

The ingots have been cut and processed using in pilot hot-rolling mill equipped with an efficient run-out table, which reaches the industrial capability in term of cooling rate. Depending on the aimed FCT given in the first column of the Table 2, the water flow inside the table has been judiciously adjusted. For each grade, different cooling conditions have been tested, with at least one condition with a FCT = 500°C. Since the temperature is measured all along the schedule using an inserted thermocouple, the cooling sequence is controlled with a high precision. As demonstrated in the table 2, the processing parameters have been followed strictly. The only noticeable discrepancy concerns the FCT of the first attempt.

The final thickness of the sheets is about 12 mm to be able to manufacture full-scale Charpy samples (10x10 mm²). Normalized cylindrical TB5 tensile samples and normalized Charpy notched samples were machined from the sheets. Fig. 3 presents the position of the samples in the steel sheets. The values given for the tensile and impact tests presented here are averaged over 3 samples. Vickers hardness testing has been carried out near the part used for microstructural investigations using a load of 30 Kg and the values presented are also averaged over 3 tests.

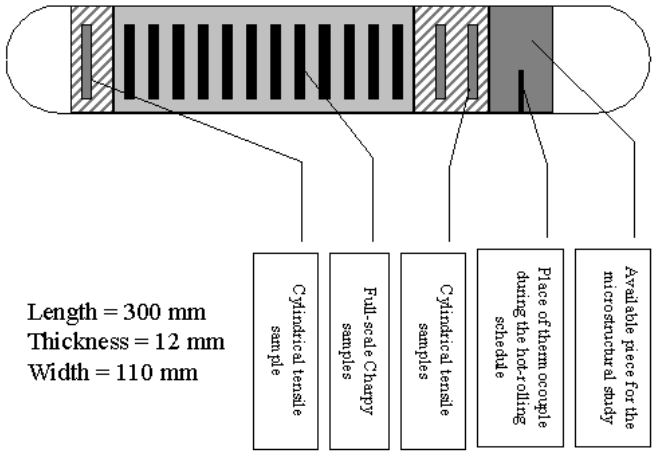

Fig. 3: Dimension of the processed thick steel sheets. The tensile and Charpy notched samples are located on the plan. Metallographic specimens are machined near the position of the thermocouple

For the microstructural study, the segments of the sheet located near the thermocouple have been used. Specimens transverse to the hot rolling direction were ground and polished using standardized techniques for metallographic examination. A 2% Nital etching solution was used to reveal the microstructure by optical microscopy. To reveal more in detail the microstructure of the steel,

scanning electron microscopy (FEG-SEM) was carried out on a Jeol JSM-6500F field emission scanning electron microscope operating at 7 kV. The volume fraction of the different phases present in the microstructure was estimated by a systematic manual point-counting procedure on optical and scanning electron micrographs.

Quantitative X-ray analysis was used to determine the fraction of retained austenite. For this purpose, 11 x 5 x 2 mm^3 samples were machined. After grinding and final polishing using 1 mm diamond paste, the samples were etched to obtain an undeformed surface. They were then step-scanned in a SIEMENS D 5000 X-ray diffractometer using unfiltered Cu-Ka radiation. The scanning speed (2q) was less than 0.3 degree/min. The machine was operated at 40 kV and 30 mA. The retained austenite content was calculated from the integrated intensities of (200), (220) and (311) austenite peaks, and those of (002), (112) and (022) planes of ferrite [18]. Using three peaks from each phase avoids biasing the results due to any crystallographic texture in the samples [19]. The carbon concentration in the austenite was estimated by using the lattice parameters of the retained austenite [20].

Specimens for transmission electron microscopy (TEM) were machined down to 3 mm diameter rod. The rods were sliced into 400 µm thick disks and subsequently ground down to foils of 50 µm thickness on wet 1200 grit silicon carbide paper. These foils were finally electropolished at room temperature until perforation occurred, using a twin-jet electropolisher set at a voltage of 40 V. The electrolyte consisted of 5 % perchloric acid, 15 % glycerol and 80 % methanol. The foils were examined in a JEOL JEM 2010 TEM at an operating voltage of 200 kV.

3. RESULTS

3.1 MECHANICAL PROPERTIES

All the results are summed up in the Table 3 for convenience. For each conditions (grades and FCT), are given the key features of the tensile tests, i.e. ultimate tensile and yield strengths, uniform and total elongation. The Charpy impact energy and Vickers hardness measured at room temperature are also indicated for assessment. To ease the interpretation of the tensile behavior, the classical product UTSxTEl and ratio YS/UTS have been calculated. The first one is useful to evaluate the resistance of the alloy for crash application whereas the second one illustrates the hardenability of the alloy during forming operations.

Table 3: Results of the tensile, Charpy and hardness tests for all the steels presented in the Table 2. (UTS = Ultimate Tensile Strength, YS = Yield Strength, UEl = Uniform Elongation, TEl = Tensile Strength, Charpy E = impact Charpy energy at 20°C, Hv = Vickers Hardness with a 30 Kg load)

References		Mechanical properties							
Grade	FCT (°C)	UTS (MPa)	YS (MPa)	UEl (%)	TEl (%)	Charpy E at 20°C (J)	UTSxTEl (MPa.%)	YS/UTS	Hv (30 Kg)
#1	500	1808	1084	4.2	11.1	36	20069	0.60	530
	600	1696	1021	3.9	10.8	22	18317	0.60	522
#2	550	1613	1132	4.1	10.3	44	16614	0.70	519
	500	1627	1020	4.7	11.6	36	18873	0.63	460
#3	550	1698	1077	4.1	10.8	46	18338	0.63	505
	500	1671	1068	4.6	12.2	44	20386	0.64	495
#4	500	1710	1097	3.6	13.9	38	23707	0.64	531
#5	550	1801	1105	4.3	11.0	31	19811	0.61	555
	500	1696	1059	4.5	11.6	40	19674	0.62	521
#6	500	1799	1074	3.9	10.7	24	19186	0.60	555
#7	500	1929	1125	4.4	9.7	25	18711	0.58	559
	600	1945	1203	3.7	7.0	26	13615	0.62	563

3.1.1 TENSILE TESTS

The tensile tests have been performed under normalized conditions, i.e. at room temperature and low strain rate. The Fig. 4 presents the results of the tensile tests for all the grades under the different conditions. The total and uniform elongations are plotted in relation with the ultimate tensile strengths. All the grades reach very high tensile strengths, above 1600 MPa while keeping a significant ductility. Slight differences are however observed between the grades and among them, Steel #7 presents the higher flow stress (about 1950 MPa) whatever the FCT. Apart from Steel #7 whose mechanical properties are obviously different, the total and uniform elongations are comparable for all the grades whatever the processing parameters and are quite impressive for such high UTS (4% and over 10 % respectively). Regarding the products UTSxTEl reached by these steels (typically 18,000 MPa.%), the properties are lower than actual ferritic TRIP steels under developments [21]. The uniform elongation of the alloys is not sufficiently high to reach better total ductility. Nevertheless, the ratio YS/UTS is low which can be beneficial for formability. The Fig. 5a presents the evolution of these properties. The measured ratios UTS/YS are quite as good as those obtained in DP steels (equiaxe ferrite and martensite as hard phase). The UTS and the hardness values are compared on the figure 5b and the classical linear relationship is verified with a factor 3.

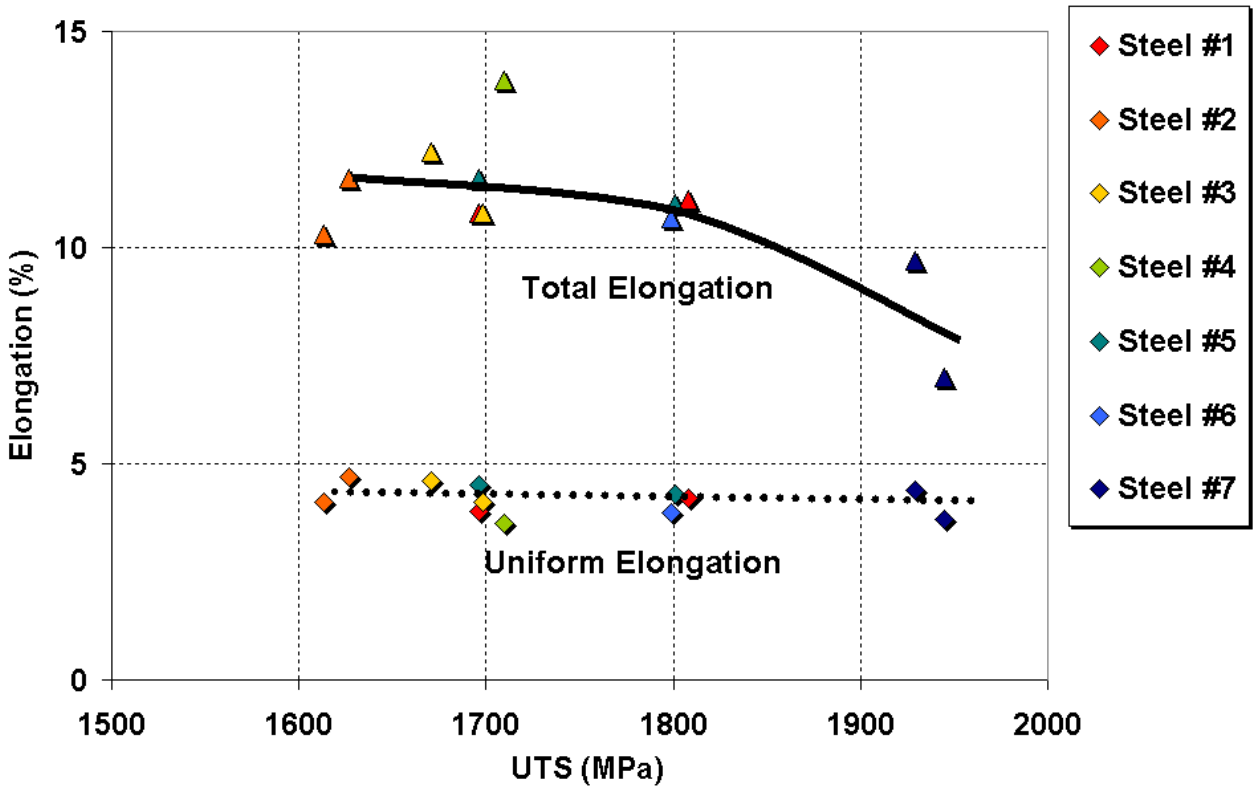

Fig. 4: Total and uniform elongations vs. ultimate tensile strengths of the steels presented in the Table 3.

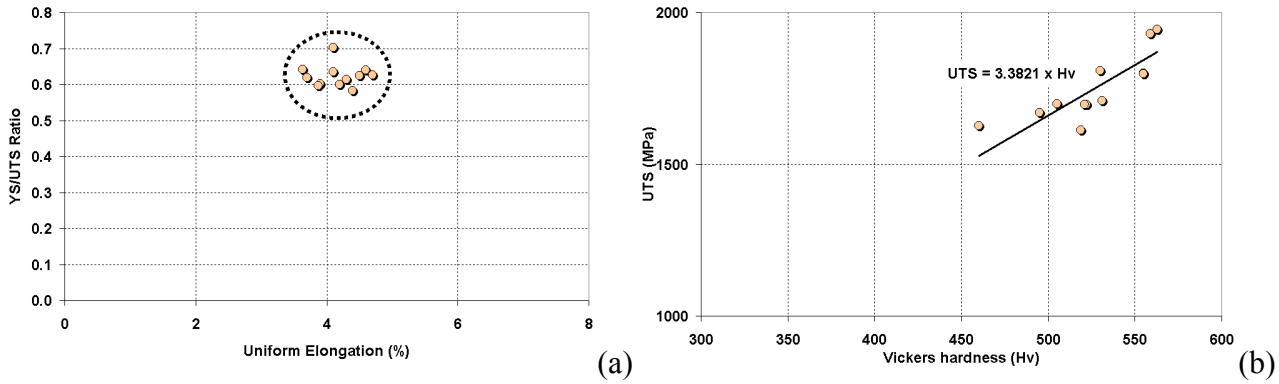

Fig. 5: Results on tensile properties (a) Measured YS/UTS vs. UEl (b) Comparison between the UTS and the Vickers hardness for the steels presented in the Table 3.

3.1.2 TOUGHNESS

The results of the Charpy tests at different temperatures are plotted on the Fig. 6. The Fig. 6a presents the values of the impact Charpy energies at room temperature in relation to the yield strength of the alloys presented in the Table 3. For the sake of comparison, the data are compared to some results proposed by Bhadeshia [2] for tempered martensite, fully bainitic steels and ferrite-pearlite steels. The toughness of the alloys designed in this study is as good as that in tempered

martensitic steels, which are known to be the best in class regarding this property. Steel #3 presents the best toughness properties and the lowest ductile-brittle transition (BDT) temperature whatever the FCT. Nevertheless, Fig. 6b shows that the BDT temperatures of the alloys are high in comparison to those in bainitic steels designed for plate's applications, for example. The results plotted on this figure only concern the alloys with a FCT = 500°C for legibility reasons. The BDT temperatures of the alloys seem to be above –20°C whatever the grade. The smooth shape of the curves is a feature of upper bainite after [2], which have been confirmed by the microstructural investigations.

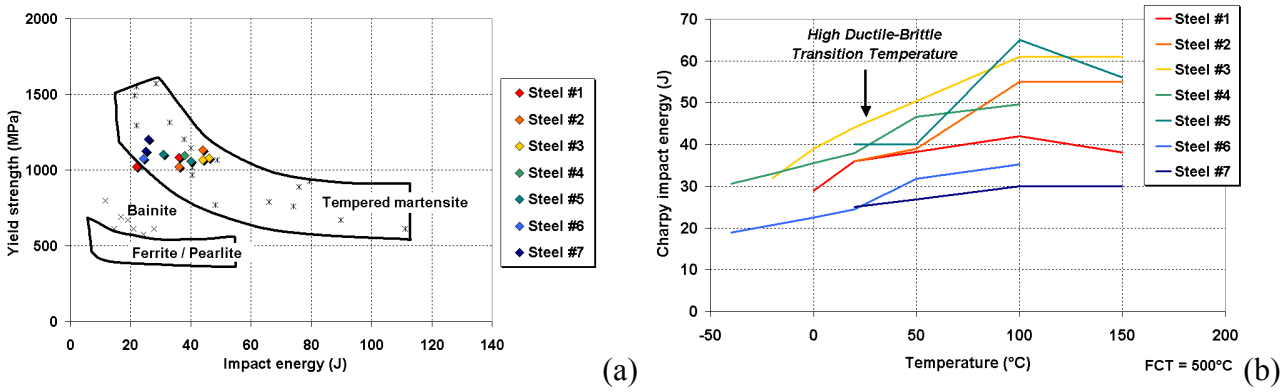

Fig. 6: Results concerning toughness properties (a) Impact Charpy energy at room temperature vs. yield strengths compared to data extracted by Bhadeshia on best-in-class hot rolled steels. (b) BDT curves for the alloy described in the Table 3 with FCT = 500°C.

3.2 MICROSTRUCTURAL INVESTIGATIONS

The results of the microstructural investigations are summed up in the Table 4 for each steel.

Table 4: Phase fractions of the bainite (B), Martensite (M) and Retained Austenite (A) in the elaborated steels after the microstructural investigations. x_c is the carbon content of the Retained Austenite.

References		Phase fraction			RA
Grade	FCT (°C)	B	M	RA	x_c
#1	500	0.73	0.24	0.03	0.66
	600	0.76	0.21	0.03	0.95
#2	550	0.77	0.13	0.10	1.14
	500	0.80	0.09	0.10	1.26
#3	550	0.86	0.03	0.11	1.04
	500	0.88	0.02	0.11	1.03
#4	500	0.88	0.09	0.03	1.26
#5	550	0.76	0.20	0.04	0.80
	500	0.81	0.10	0.08	1.18
#6	500	0.86	0.07	0.07	1.60
#7	500	0.62	0.30	0.09	0.98
	600	0.56	0.39	0.05	0.75

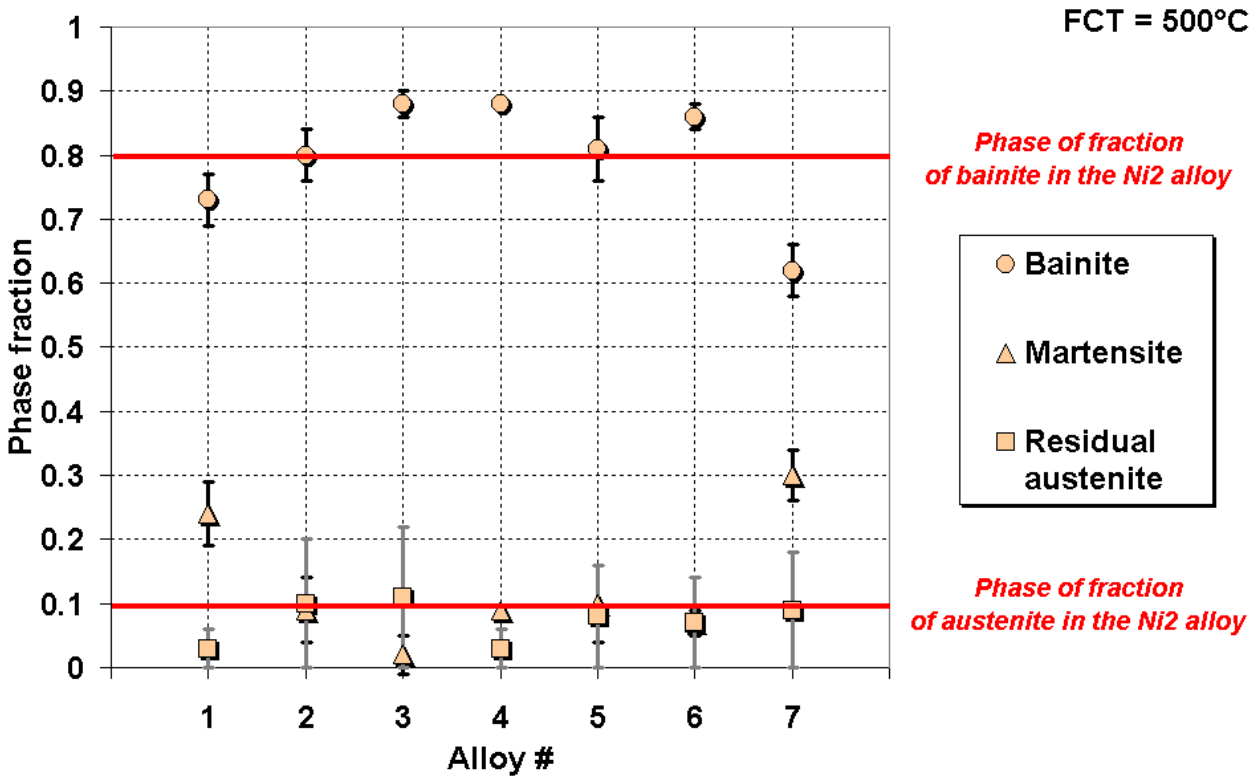

Fig. 7: Phase fractions in the different alloys. The scattering bars are calculated depending on the measurement method for each phase. The bainite and austenite contents in the Ni2 reference alloy are drawn for the sake of comparison.

Microstructural characterization revealed that Steels # 1, 2, 3, 4, 5 & 6 after air cooling from every temperature tested have the desired microstructure consisting of carbide-free upper bainite (See optical micrographs in Fig 8.). Due to the high volume fraction of bainitic ferrite in those samples, more than 0.75, retained austenite is present as films between the subunits of bainitic ferrite free of carbides (See TEM micrographs in Fig. 9a as an example). TEM micrographs also confirm the absence of carbides in the bainitic microstructure apart from a few sheaves of lower bainite with fine carbides precipitated inside ferritic plates observed in Steel #5. The small amount of bainite in Steel #7 after air-cooling causes much of the residual austenite to transform to martensite during cooling because of lower carbon enrichment. An example of blocky tempered martensite in this steel is shown in Fig. 9b where the typical multi variant carbide precipitation is observed.

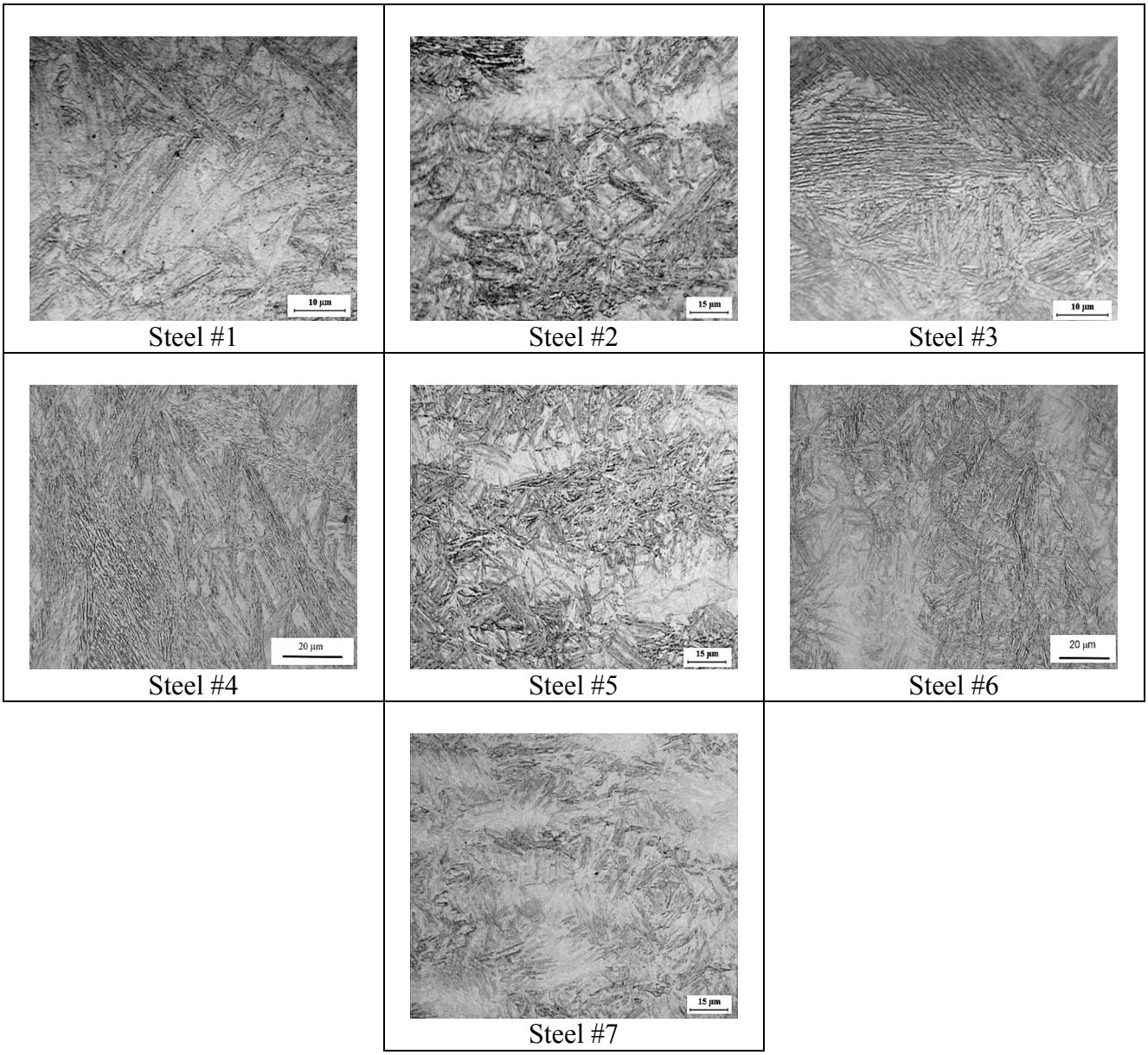

Fig. 8: Optical micrographs of the different steels with FCT = 500°C. Grain and bainitic lath boundaries are revealed by Nital etching. The references of the steel and the scales are given for each micrograph.

As a conclusion, all the designed steels contain more or less the same expected fraction of carbide free upper bainite apart form Steel #7 in which the bainitic transformation is probably slowed down by the highest amount of alloying elements. It is also noteworthy that the amount of phases in the successful tries is quite comparable to those measured in the Ni2 steel, which is the primary goal of the study.

Preliminary optical examinations of the samples revealed the presence of bands in the microstructure. Hardness measurements on the transversal sections show no difference between the center and the surface of the samples. This micro-heterogeneity problem has thus no consequence on the reliability of the mechanical tests. Nevertheless, these defects in the microstructure, which are probably due to the low reduction in thickness during hot rolling, could have negative impact on formability and bendability.

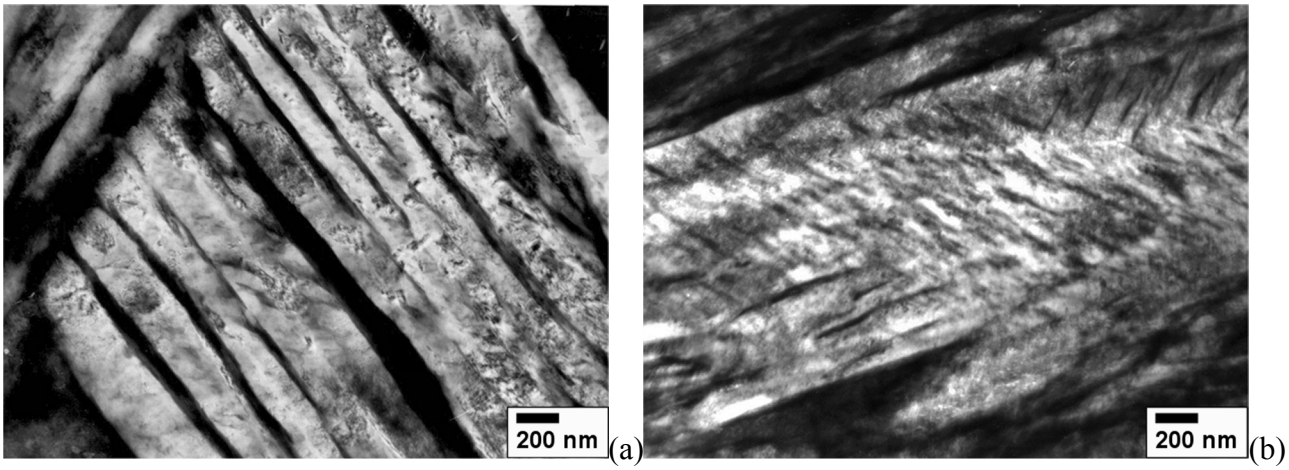

Fig. 9: TEM bright field micrographs: (a) Carbide-free upper bainitic microstructure in Steel #5. Bainite laths appear in clear whereas retained austenite between the ferrite plates is out of contrast. (b) Block of tempered martensite in Steel #7. The multi-variant carbides appear in dark.

3.3 DISCUSSION

The Fig. 10 presents the evolution of the mechanical properties of the steel in relation with the specific amount of each main alloying element. The data concerning Steel #7 have not been reported since its microstructure is obviously distinct. No distinctions have then been made between the remaining alloys. The alloy design is based on the concept that modifying the amount of a given alloying element can be compensated by the modifications of the others contents to keep the thermodynamic properties unchanged. As expected, the figure shows that none of the elements present an individual effect on the mechanical behavior. The only origin of scattering is the effect of changing the processing parameters (FCT). Steel #7 is the alloy with the higher content of alloying elements. The interactions between Al, Co, Ni and Cr have probably induced effects not taken into account or underestimate in the modeling and lead to the slowest bainitic transformation.

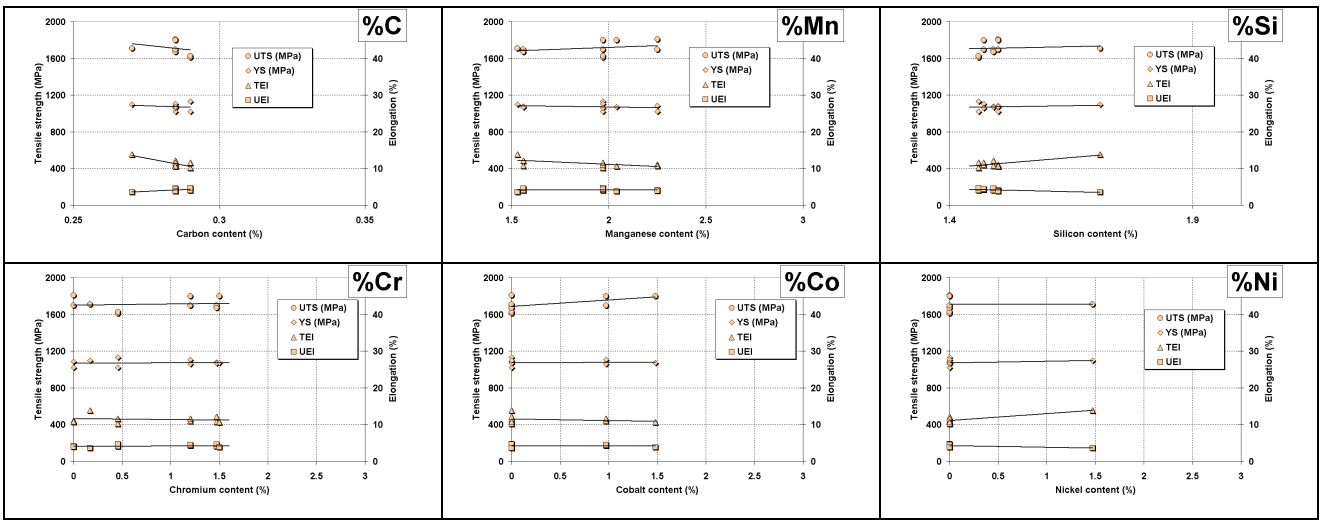

Fig 10: Effect of alloying elements on the mechanical properties of the steels whose microstructure is composed of carbide-free upper bainite, i.e. all the designed steels except Steel #7.

The most unexpected result of the study is the low YS/UTS ratio measured on these bainitic steels, which is more often a distinguishing quality of DP steels. In these particular steels, the high hardening rate is due to a composite effect, i.e. a very dissimilar mechanical behavior of martensite and ferrite. The tensile curves of the studied steels do not even present a perceptible TRIP effect. It seems that the retained austenite in the Martensite-Austenite blocks is not sufficiently stable to transform slowly along with strain. The austenite to martensite transformation occurs swiftly and the effective microstructure from a micromechanical point of view is mainly composed of bainite and martensite in the studied steels leading to a kind of DP effect. This explanation is supported by the low carbon content measured in those steels (See Table 4). Nonetheless, it seems unrealistic that the austenite films between bainite laths participate to the phenomena. Only blocky regions of austenite may transform to high carbon, untempered martensite under the influence of small stresses. This transformation is known to have an embrittling effect [6,22] As a consequence, future works will consist in analyzing the microstructure after a tensile deformation to check our conclusions.

4. CONCLUSIONS

An innovative concept based on theory alone has been followed to design new hot-rolled bainitic steels free of carbides. The master idea is to adapt their compositions to reproduce the thermodynamical behavior, and thus the microstructure of given steel, which appears to be a benchmark for mechanical properties but not adapted for automotive purposes. Seven alloys have been proposed after calculation and processed using the same hot-rolling schedule at the semi industrial scale.

Except for the steel with highest content of alloying element (Steel #7), all the grades present the same microstructure composed of carbide-free upper bainite, retained austenite and blocks of tempered martensite. As expected, the studied steels present quite similar significant combinations of strength and ductility. Theirs tensile strengths range from 1600 MPa to 1950 MPa while keeping a uniform elongation equal to 4 % and a total elongation over 10 %. Regarding toughness at room temperature, they match quenched and tempered martensitic steels. The DBT temperature is quite high but the transition smooth due to the microstructure mainly composed of upper bainite. It appears that the alloys present a low YS/UTS, which is probably due to an insufficient carbon enrichment of the retained austenite during bainitic transformation. The ductility of the alloys can still be improved. Finally, it has been demonstrated that steels present a low sensivity to processing parameters. The alloy design is thus a success not only from the microstructural point of view but also from mechanical results.

ACKNOWLEDGEMENTS

The authors gratefully acknowledge the support of the Research Fund for Coal and Steel for funding this research under the contract 7210-PR/345. M.J. Santofina would also like to express her gratitude to Consejo Superior de Investigaciones Cientìficas (CSIC) for the financial support in the form of a PhD Research Grant (I3P Program). We also want to thank the other contributors of the

project, H. Spindler (Voestalpine) and Prof. S. Zajac (KIMAB) for our fruitful discussions about bainitic transformations.

REFERENCES

1) T. ARAKI, E. MASATO and K. SHIBATA, Mat.Trans. 32, (1991), p.729.
2) H.K.D.H. BHADESHIA, Bainite in Steels, Second Edition. IOM Comunications, London (1992).
3) Patent JP 2004332099, Nippon Steel Corporation, (2004).
4) ECSC Technical Report No. 5 Contract No. 7210-PR-345, (2004).
5) ECSC Technical Report No. 2 Contract No. 7210-PR-345, (2003).
6) H.K.D.H. BHADESHIA and D.V. EDMONDS, Metal.Sci. 17, (1983), p.411.
7) H.K.D.H. BHADESHIA and D.V. EDMONDS, Metal.Sci. 17, (1983), p.420.
8) V.T.T. MIIHKINEN and D.V. EDMONDS, Mater.Sci.Technol. 3, (1987), p. 422.
9) V.T.T. MIIHKINEN and D.V. EDMONDS, Mater.Sci.Technol. 3, (1987), p. 432.
10) V.T.T. MIIHKINEN and D.V. EDMONDS, Mater.Sci.Technol. 3, (1987), p. 441.
11) F.G. CABALLERO, H.K.D.H. BHADESHIA, K.J.A. MAWELLA, D.G. JONES and P. BROWN, Mater.Sci.Technol. 17, (2001), p. 512.
12) http://www.msm.cam.ac.uk/map: Materials Algorithms Project (MAP), University of Cambridge, Department of Materials Science and Metallurgy.
13) H.K.D.H. BHADESHIA, Acta.Metall. 29, (1981), p. 1117.
14) H.K.D.H. BHADESHIA and A. R. WAUGH, Acta Metall. 30, (1982), p. 775.
15) L.C. CHANG and H.K.D.H. BHADESHIA, Mater.Sci.Eng.A 184, (1994), p. 17.
16) I. STARK, G.D.W. SMITH and H.K.D.H. BHADESHIA, Solid→Solid Phase Transformations, Institute of Metals, London (1988), p. 211.
17) C. GARCIA-MATEO, F.G. CABALLERO and H.K.D.H. BHADESHIA, ISIJ Int. 43, (2003), p. 1821.
18) J. DURNIN and K.A. RIDAL, J.Iron.Steel.Inst. 60, (1968); p. 206.
19) M.J. DICKSON, J.Appl.Cryst. 2, (1969), p. 176.
20) D.J. DYSON and B. OLMES, J.Iron.Steel.Inst. 208, (1970), p. 469.
21) P. JACQUES, A. PETEIN and P. HARLET, Proc.1st.Int.Conf.TRIP-aided High Strength Ferrous Alloys, Ghent (2002), GRIPS, Bad Harzbourg, Deutschland (2002), p. 281.
22) H.K.D.H. BHADESHIA, Mater.Sci.Technol. 15, (1999), p. 22.